Nanozole: a proposed nanotherapeutic formulation for the treatment of ocular *Baylisascaris procyonis* infection

uOttawa

Faculté de médecine
Faculty of Medicine

J. Cuthbert,[a†] L. Vukovic,[a†] E. Alarcon,[a] and S. Gadde[a]

Received (in online submission) 17th December 2019

Baylisascaris procyonis (*B. procyonis*) is a ringworm capable of infecting the eye and parts of the central nervous system. The current standard treatment for ocular infection is oral administration of Albendazole, a broad-spectrum anthelmintic, and laser photocoagulation. Despite these treatments, the prognosis for *B. procyonis* patients with ocular infection remains poor. Uptake of systemic Albendazole is low and laser photocoagulation is inaccessible for patients in developing countries, where infection is more common. We propose a novel nanotherapeutic approach as a supplemental treatment for ocular *B. procyonis* infection - a polymeric micelle system capable of delivering Albendazole across the eye and into the vitreous humor for targeted anthelmintic activity. This paper outlines the proposed experimental approach for synthesizing and characterizing Albendazole-loaded polyethylene glycol-modified poly(lactic-co glycolic acid) (PEG-PLGA) nanoparticles, referred to as Nanozole. We also outline in-vitro and in-vivo efficacy tests and a commercialization strategy for marketing Nanozole. Through our work we hope to improve Albendazole delivery to the eye, reduce side effects, and improve the outcome for *B. procyonis* patients globally.

1. Introduction

Baylisascaris procyonis (*B. procyonis*) is a roundworm found across the Americas, Europe and Japan (1). They are known to infect racoons, rats and canines (1). While rare, they are capable of infecting human children (1). They typically enter via oral ingestion (2). Once inside, larva migrans penetrate the gut wall and enter circulation (2). From here, they infect the central nervous system, disrupt hepatic portal circulation and enter the vitreous humour (VH) of the eye (2). This leads to marked neurological defects, hepatomegaly and various ocular concerns including unilateral nystagmus and, sometimes, blindness (2). The standard treatment for *B. procyonis* infection involves doses of the broad-spectrum anti-helminthic Albendazole and corticosteroid administration (2). For ocular infection, laser photocoagulation may also be used (1,2). Despite the current available treatments, prognosis remains poor and the eye can be severely damaged or lost.

One challenge in treating ocular *B. procyonis* infection is efficient ocular drug delivery. Currently, Albendazole is administered as a pill (2). However, the uptake of drugs into the eye from systemic circulation is low (3). As such, the infection may persist longer in the VH. Another challenge is the lack of access to photocoagulation patients may face. Countries with lower sanitation levels, where roundworm infection is especially common, often lack the resources for laser therapy (4). Together, this means there is a large gap in the global market for effective treatment of ocular *B. procyonis* infection.

Nanomedicine-based therapies are a viable avenue for treating ocular infections. There have been many recent advancements made in nano-based ocular drug delivery systems. Ballesteros et al., for example, designed a novel hybrid liposome vehicle for glaucoma (5). Another group demonstrated that levofloxacin-loaded nanoparticles (NPs) can kill bacteria in the eye (6). Polyethylene-glycol modified poly(lactic-co glycolic acid) (PEG-PLGA) NPs are a promising synthetic polymeric micelle for ocular drug delivery, since they present low cytotoxicity levels and have been demonstrated to enter the eye (7,8). Despite these recent advancements, there have been no reported attempts to make an ocular-compatible anthelmintic or anti-*B. procyonis* NP system.

Our group proposes a PEG-PLGA-based NP system for eye-drop delivery of Albendazole to supplement ocular treatment for *B. procyonis* infection. We propose steps to synthesize and characterize Albendazole-loaded PEG-PLGA NPs, as well as a biocompatible delivery medium. Next we outline how we intend to test the system in cultured ocular epithelial cells and in a rabbit model of *B. procyonis* infection. We also describe our plan to compare ocular uptake from free Albendazole compared to NP-based delivery. Lastly, we outline a commercialization strategy to market our proposed therapeutic system, which we refer to as Nanozole. Based on previous research, we anticipate improved delivery and reduced systemic effects with Nanozole.

2. Proposed Methods & Expected Outcomes

2.1 Preparation and characterization of Albendazole loaded PEG-PLGA NPs.

To synthesize the PEG-PLGA micelles, we propose using a standard nanoprecipitation synthesis method, as outlined by Cheng et al. (9). Briefly, PEG-PLGA

copolymer and Albendazole are dissolved in dimethylformamide (DMF). This solution is added dropwise to nano-filtered water, where the polymers self-assemble into micelle structures. Figure 1 demonstrates the assembly of polymeric micelles via nanoprecipitation as well as the anticipated micelle structure.

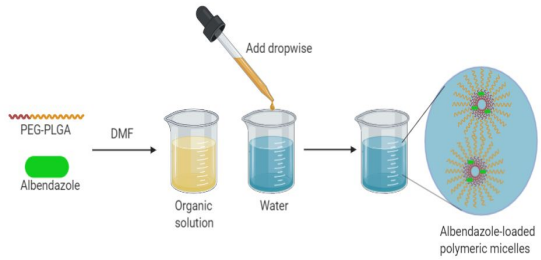

Fig 1. Nanoprecipitation for synthesis of Albendazole-loaded PEG-PLGA NPs. PEG-PLGA and Albendazole are dissolved in DMF and added dropwise to water, where they self-assemble into drug-loaded NPs. Based on the method outlined by Cheng et al. (9). Prepared by J. Cuthbert.

Based on previous research, we expect spherical NPs with an average diameter ranging from 130 to 200 nm (9). We also expect low polydispersity and limited heterogeneity (9). These are important for consistent drug loading and because, according to Vega et al., NPs around 200nm are ideal for ocular penetration (24). However, research is somewhat contradictory on PEG NP morphology, so we would have to assess these properties with transmission-electron microscopy (TEM) and dynamic light scattering (DLS). Figure 2 demonstrates a TEM-captured image of spherical PEG-PLGA NPs and a hydrodynamic diameter distribution graph obtained with DLS, originally published by Xialong et al. in 2015 (10).

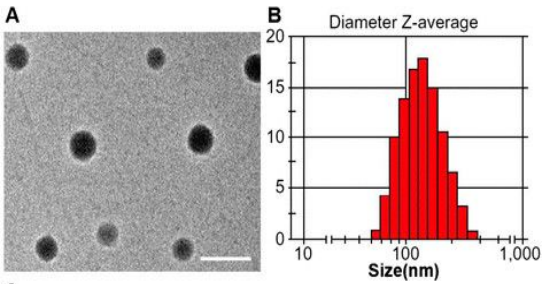

Fig 2. PEG-PLGA NPs are spherical with an average diameter of 136nm. Adapted from Xiaolong et al., 2015 (10). A: TEM image shows spherical NPs with low polymorphism. Scale bar represents 200nm. B: Hydrodynamic diameter distribution acquired via DLS. Samples were measured using the Malvern Zetasizer 2000. Average diameter is 136 nm, average PDI 0.13±0.005. Prepared by J Cuthbert.

PEG-modified NPs tend to have a neutral surface charge with a low zeta potential and limited surface corona interactions (11). We can measure the zeta potential using a zetasizer, such as the Malvern Zetasizer 2000. Table 1 demonstrates expected zeta potentials for PEG-PLGA NPs, based on work published by Pamujula et al. in 2013 (11).

Table 1. PEGylated PLGA NPs have a lower zeta potential compared to PLGA NPs. Adapted from Pamujula et al., 2013 (11). PLGA and 15% PEG-PLGA NPs were assessed using the Malvern Zetasizer 2000. PEG-PLGA NPs show a lower zeta potential and increased cellular uptake. Prepared by J. Cuthbert.

Formulation	Particle size and range (90th percentile, nm)	Zeta Potential (mV)[a]
PLGA (without PEG)	210 (85-353)	-26.24±5.2
PLGA (with 15% PEGylated PLGA)	114 (73-324)	-2.8±1.60

[a]Each reading represents the mean of triplicate samples ± SD.

The presence of a surface corona, dictated by the surface charge, determines how NPs interact with biomolecules and their effectiveness in drug delivery. TEM can be used to determine the presence of a surface corona, while high-performance liquid chromatography with mass spectrometry (HPLC-MS) can be used to analyse the composition of said corona. It is important the corona be characterized in our delivery medium as well as the VH, since it can differ depending on the solution. Figure 3 demonstrates this using gold NPs in two different serums. It also demonstrates typical results from HPLC-MS analysis. Figure 3 was created using data published by Stewart et al. in 2018 (12).

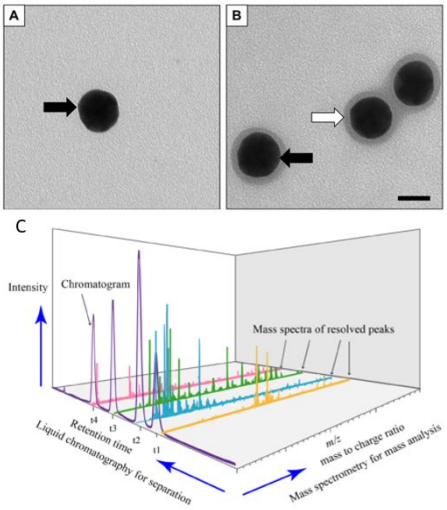

Fig 3. Surface coronal composition differs depending on the solution and surface charge of NPs. A: Gold NPs in protein free serum. B: Gold NPs in serum containing various proteins. C: Diagram demonstrating HPLC-MS results and how to interpret them. Figure created with data from Stewart et al., 2018 (12) and with a diagram from Wikimedia commons. Prepared by J. Cuthbert (2019).

Given their expected neutral surface charge, we expect minimal interaction with proteins in our delivery medium and in the VH, however we would

have to test this in both solutions.

2.2 Measurement of Encapsulation Efficiency

To quantify Albendazole loading in the micelles, we will follow a protocol outlined by Wijesooriya et al., where they assessed drug loading in liposomal NPs (13). First, we will isolate particles from solution by centrifuging them over a filter that traps particles the same size as our NPs in kDa - much like size-exclusion chromatography. We will then wash them to remove any free drug. Next, to calculate the encapsulation efficiency, we will use Basavaiah and Prameela's method for estimating Albendazole content in dosage forms via spectrophotometric analysis (14). Briefly, the isolated particles will be emulsified to expose their PLGA interiors and the encapsulated Albendazole. We would incubate the solution with chloramine-T, which acts as an oxidimetric reagent and reacts with Albendazole to produce a colometric reaction. This allows for spectrophotometric analysis and for us to estimate Albendazole concentration up to $1.15\ \mu g/ml$.

2.3 Development of the Eye Drop Formulation

An appropriate delivery solution needs to consider patient safety, long-term NP stability and have limited impact on the drug's pharmacokinetic capabilities. For safety, a solution based on natural human teardrops and current market teardrop solutions would make for a conservative and simple approach. Tears typically have an organic, aqueous, and protein component (22). Due to the amphiphilic nature of the PEG-PLGA NPs, the organic component will be excluded from our solution, in order to maximize NP stability. The aqueous component would ideally mimic plasma salt concentrations, similar to popular synthetic teardrop brands like *Refresh Tears* by Allergan (18). The protein component can increase solution viscosity and NP adsorption to the corneal epithelium, which itself is typically covered in a thin layer of mucin.

Next, the solution has to ensure NP stability. When considering the rarity of *B. procyonis* infection, our eye-drops need to have a long shelf life. One option would be to increase the hydrophobicity of the interior copolymer by increasing the PLGA copolymer length, thereby increasing cohesion and thermodynamic stability. The solution's pH and salt concentrations can also be manipulated to maximize NP longevity. Lastly, our solution has to consider pharmacokinetic properties. Studies have shown viscosity enhancers, such as methyl cellulose, can increase our solution's residency time in the precorneal area (19,20). This maximizes NP corneal adsorption and, consequently, entry into the eye.

2.4 In-vitro: Cell Viability Experiments

A report by Lin *et al.* where they incubated ocular epithelial cells for 6 days with high concentrations of PEG-PLGA NPs demonstrated they have little to no cytotoxicity (15). They use this as evidence to suggest PEG-PLGA NPs are a viable ocular delivery system. Nonetheless, we plan to repeat their experiments to validate Nanozole's safety. In one experiment we will use ocular epithelial cells in a Live/Dead assay to calculate toxicity levels. Next, a shrimp luciferase assay will be used to explore metabolic states in ocular epithelium cells treated with the NPs. This test uses a luciferase enzyme to catalyze the formation of fluorescent light from substrates generated by metabolically active cells. Since the light is proportional to substrate concentration, a stronger signal suggests more metabolically active cells. Both experiments will use a double negative control (no drug, no particle), a negative control (empty NPs), a positive control (free albendazole exposure), and an experimental group (Nanozole). We expect no cytotoxicity until perhaps Albendazole concentrations exceed tolerable limits set by TD50 concentrations.

2.5 In-vitro: Efficacy Experiments

To test the therapy's effectiveness, we will treat cultured *B. procyonis* worms with various concentrations of either empty NPs, free drug or Nanozole. Through this we can establish a working concentration for in-vivo experiments and demonstrate the efficacy of the therapeutic. We anticipate similar anthelmintic activity between the free drug and Nanozole. However, while it should not affect its therapeutic potential, there is the possibility of a delay in the nanotherapy-based killing, since the NPs need to degrade for drug release. Figure 4 demonstrates the proposed workflow and results for these experiments.

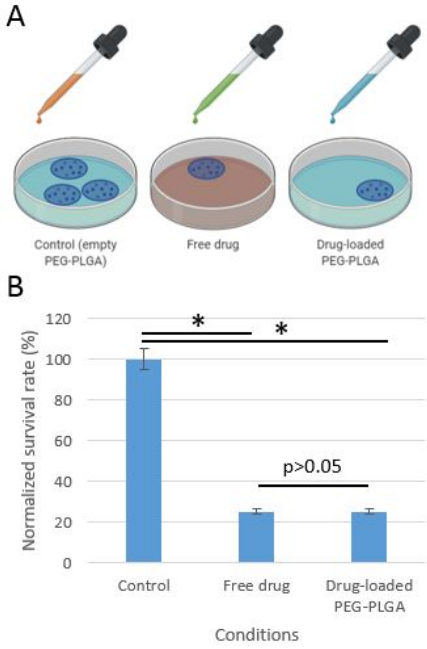

Figure 4. Albendazole-loaded PEG-PLGA NPs will have similar anthelmintic activity as free drug. A: Experimental workflow. Cultured *B. procyonis* will be treated with either empty PEG-PLGA NPs, free Albendazole or Albendazole-loaded PEG-PLGA NPs at various concentrations.

B: Worm survival rates for different conditions. Drug-loaded PEG-PLGA NPs should have the same efficacy as the free Albendazole. n=3, *=p<0.05. Prepared by J. Cuthbert.

2.6 In-vivo: Establishing an Animal Model

One limitation is the lack of an established animal model for ocular *B. procyonis*. Furuoka et al. report that rabbits are susceptible to infection by the roundworm (16). They could serve as an effective model for a number of reasons. First, they have similar corneal morphology to human eyes, and are commonly used in preclinical ocular pharmacokinetic studies, at outlined by Agrahari *et al.* in 2016 (21). We need to partner with another group to validate this model (see "Commercialization Strategy"). While more expensive than a typical mouse model, the rodent's ocular anatomy and corneal structure deviates too far from human corneas, preventing it from being a viable model. To validate our safety tests in another animal, pigs could be useful. Their eyes are remarkably similar to humans' and, moreover, corneal xenografts are typically derived from pigs, suggesting their usefulness as a model system for human ocular disease (23).

2.7 In-vivo: Pharmacokinetic Characterization of PEG-PLGA nanoparticle ocular penetration.

Pharmacokinetics will be evaluated with rabbits and simulated models. Prior to animal testing, we will use a compartmental model to estimate the rate at which PEG-PLGA particles can reach the VH. When paired with particle degradation rates, we can estimate where Albendazole will be localized during different stages of treatment. Briefly, the compartment model assumes homogeneous drug distribution in each region. Since there are 5 areas through which the particles travel - the precorneal area, cornea, aqueous humour, lens, and VH - we will utilize a 5 compartment model for our estimations. Based on Fick's law and the four possible permeability barriers our simulations will be modelled by the following four equations:

1) $\frac{dC_p}{dt} = K_{pc}\,A\,(C_p - C_c)$ *Pre-cornea to cornea*
2) $\frac{dC_c}{dt} = K_{c\,ah}\,A\,(C_c - C_{ah})$ *Cornea to aq. humour*
3) $\frac{dC_{ah}}{dt} = K_{ah\,l}\,A\,(C_{ah} - C_l)$ *Aq. humour to lens*
4) $\frac{dC_l}{dt} = K_{lv}\,A\,(C_l - C_v)$ *Lens to vitreous humour*

where C_p is precorneal concentration, C_c is corneal concentration, C_{ah} is aqueous humour concentration, C_l is lens concentration, C_v is vitreous humour concentration, A is contact area, and K is the permeability constant across two compartments. All equations model compartment particle concentrations as a function of time. Figure 5A demonstrates the 5-compartment model of the eye.

We expect Albendazole release to be delayed by the half life of the PEG-PLGA particles, which Rafiei et al. found to be about 15 hours (18). This is useful, since it offers several hours for the particles to diffuse to the VH before breaking down. To test diffusion rates in-vivo, fluorescent NPs can be administered to our rabbit model, and the VH can be sampled via intravitreal micro-aliquot aspirations at consistent time points. Fluorescence HPLC can be used to assess particle concentration in the micro-aliquots, and HPLC or spectrophotometric analysis (as outlined in section 2.2) can quantify Albendazole concentration in the VH. Figure 5B shows our expected results.

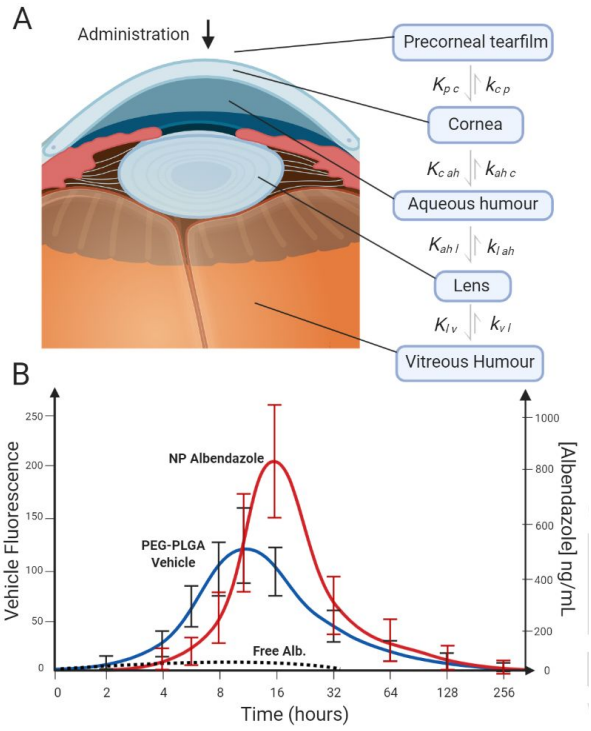

Fig. 5. 5-compartment model of the eye and expected results from VH micro-aliquot analysis. A: Schematic of the 5-compartment model. B: Nanozole VH penetrability and VH Albendazole concentrations over time. Rabbits are treated with the fluorescein labelled vehicle and either Nanozole or free drug. Micro-aliquot aspirations of the VH are taken and analyzed via fluorescence HPLC and HPLC to characterize delivery rates. We expect a 62x area under the curve (AUC) improvement with Nanozole compared to free drug. n=4, p<0.001. Prepared by L. Vukovic (2019).

Lastly, since we want to lower systemic drug exposure and improve ocular specificity, we plan to collect blood samples during and post eye-drop administration, and quantify Albendazole levels. This will tell us if the NPs effectively limit systemic drug circulation.

3. Commercialization Strategy

Research and development should be the shortest phase of commercialization. Particle development strategies are already well established, meaning we only have to optimize. We plan to partner with another pharmaceutical group to validate our rabbit

model, so we can focus on this. In total we expect development to last 3 months and ex-vivo testing about 9. Animal testing should begin September 2020 and last until winter 2021. If results are promising and funding is available, we hope to move on to porcine models, in order to validate our delivery system in two different systems.

Assuming promising outcomes, drafting and the first-filing of a product patent should take about 2 and 12 months respectively. Since we aim to apply the product on a global scale we would file via PCT to monopolize technology rights in all relevant countries, budget permitting. To prioritize countries where we should patent first we would look for comparable market competition and epidemiological factor - i.e. countries where the infection is most rampant. This could take up to 18 months, with the entire process taking up to 3 years. It would be key to begin this prior to clinical trials. We expect early phase clinical testing to start mid-2021 following in-vivo validation. Phase 1 would test for empty particle safety and Albendazole particle safety on two different groups (n=[10,20] each). After phase 1 safety testing we expect recruitment for phase 2-3 trials (n=[40,80]) to last several months. The formulation is not aimed towards systemic infections with *B. procyonis* so will need to be validated as a supplement to current treatment standards. Proving improvements in prognosis via a supplemental treatment may be difficult in consideration of the already poor prognosis, thus ocular parasitic clearance would be an essential variable to assess.

Successful patent filing and clinical trials marks when Nanozole would be founded. NanoAssemblr® microfluidic technology by Precision Nanosystems is a polymeric nanoparticle scale-up solution in place for the manufacturing process of Nanozole that includes preparation, storage, purification, sterilization, and custom concentration adjustment of PEG-PLGA particles. While partnered with Starfish Medical, outreach and industry engagement would let us access a global market with a cost-effective, high patient adherence, portable, and accessible treatment solution.

In later commercialization phases, or if explorative outcomes suggest an exigency to pivot formulation objectives, our developed particle can still serve a multitude of other uses as: a drug substitution vehicle for other pathologies, a contact lense component for chronic treatment plans, and even as an antibody linking system for extremely precise molecular targeting. We believe in Nanozole's potential to significantly improve the lives of the vulnerable globally, particularly in regions that may not have advanced imaging or expensive laser coagulation treatment options for ocular infections. With high translatability, an investment with Nanozole is the first step to a future with post-modern polymeric nanoparticle drug formulation technologies.

Author contributions

JC prepared Fig. 1-4, Table 1, the introduction & sections 2.1, 2.4, 2.5 and 2.6. LV prepared Fig. 5, sections 2.2, 2.3, 2.4, 2.6, 2.7 & the commercialization strategy. Both authors contributed to the abstract.

Acknowledgments

We would like to thank N. Travis, S. Dhaliwal, E. Alarcon & S. Gadde for their feedback & training. We also thank BioRender for their figure design software.

Notes and references

1. K. Kazakos, L. Jelicks, H. Tanowitz, *Handbook of Clinical Neurology*, 2013, **114**, 251.
2. A.D. Sicar, F. Abanyie, D. Blumberg, et al., *Morbidity and Mortality Weekly Report*, 2016, **65,** 930.
3. B. Yavuz, U.B. Kompella, *Handbook of Experimental Pharmacology*, 2017, **242**, 57.
4. M. Muqit, S. Aldington, P. Scanlon, *Retina*, 2019, **39**, 1430.
5. M.G. Ballesteros, J.L. Cano, I.B. Osuna, et al., *Polymers (Baseline)*, 2019, **6**, 929.
6. Ameeduzzafar, S.S. Imam, S.S. Abbas Bukhari, *International Journal of Biological Macromolecules*, 2018, **108**, 650.
7. H.Lin, Y. Yan, D.E. Maidana, et al., *Seminars in Ophthalmology*, 2016, **31**, 1.
8. R.G. Pizarro, G. Parrotta, R. Vera, et al., *Nanomedicine*, 2019, [epub ahead of print].
9. J. Cheng, B.A. Teply, I. Sherifi, et al., *Biomaterials*, 2007, **28**, 869.
10. X. Tang, Y. Liang, X. Liu, et al., *Nanoscale Research Letters*, 2015, **10**, 413.
11. S. Pamujula, S. Hazari, G. Bolden, et al., *Journal of Pharmacy and Pharmacology*, 2013, **64**, 61.
12. M. Stewart, M.R. Mulenos, L.R. Steele, et al., *Applied Science*, 2018, **8**, 2669.
13. C. Wijesooriya, M. Budai, L. Budai, et al., *Journal of Basic Clinical Pharmacology*, 2013, **4**, 73.
14. K. Basavaiah, H. Prameela. *Societa Chimica Italiana*, 2003, **58**, 527.
15. H. Lin, Y. Yue, D.E. Maidana, et al., *Seminars in Ophthalmology*, 2016, **31**, 1.
16. H. Furuoka, H. Sato, M. Kubo,et al., *Journal of Veterinary Medical Science*, 2003, **65**, 695.
17. P. Rafiei, A. Haddadi, *International Journal of Nanomedicine*, 2017, **12**, 935.
18. Allergan Inc., *eyemedsnow.com*, 2018. https://bit.ly/38LyxL2
19. G. Meseguer, P. Buri, B. Plazonnet, et al., *Journal of Ocular Pharmacology*, 1996, **12**, 481.
20. B.M. Gebhardt, E.D. Varnell, H.E. Kaufman, *Journal of Ocul Pharmacol*, 1995, **11**, 509.
21. V. Agrahari, A. Mandal, V. Agrahari, et al., *Drug Delivery & Translational Research*, 2016, **6**, 735.
22. M. Joshirfar, K. Pierson, K. Hanamaikai, et al., *Clinical Ophthalmology*, 2014, **8**, 1419.
23. S.Abhari, M. Eisenback, H.J. Kaplan, et al., *Anatomical Record*, 2018, **301**, 1955.
24. E. Vega, M.A. Egea, O. Valls, et al., *Journal of Pharmaceutical Sciences*, 2006, **95**, 2393.